IEEE Access
Multidisciplinary | Rapid Review | Open Access Journal

Received May 29, 2021, accepted June 19, 2021, date of publication June 28, 2021, date of current version July 26, 2021.

Digital Object Identifier 10.1109/ACCESS.2021.3092704

A New Paradigm in 5G Maximum Power Extrapolation for Human Exposure Assessment: Forcing gNB Traffic Toward the Measurement Equipment

MARCO DONALD MIGLIORE[1,2,3], (Senior Member, IEEE), DANIELE FRANCI[4], SETTIMIO PAVONCELLO[4], ENRICO GRILLO[4], TOMMASO AURELI[4], SARA ADDA[5], RICCARDO SUMAN[6], STEFANO D'ELIA[6], AND FULVIO SCHETTINO[1,2,3], (Senior Member, IEEE)

[1]Dipartimento di Ingegeria Elettrica e dell'Informazione "Maurizio Scarano" (DIEI), University of Cassino and Southern Lazio, 03043 Cassino, Italy
[2]ELEDIA Research Center (ELEDIA@UniCAS—University of Cassino and Southern Lazio), 03043 Cassino, Italy
[3]National Inter-University Consortium for Telecommunications (CNIT), 43124 Parma, Italy
[4]Agenzia per la Protezione Ambientale del Lazio (ARPA Lazio), 00172 Rome, Italy
[5]Dipartimento Rischi Fisici e Tecnologici, Arpa Piemonte, 10015 Ivrea, Italy
[6]Group Network, Mobile Access Engineering, Vodafone Italia SpA, 10015 Ivrea, Italy

Corresponding author: Fulvio Schettino (schettino@unicas.it)

This work was supported in part by the Ministry of Instruction, University and Research under Grant Dipartimenti di Eccellenza (2018-2022), and in part by the Project of Relevant National Interest (PRIN) through Project Multilevel methodologies to investigate interactions between radiofrequencies and biological systems (MIRABILIS) under Grant 2017SAKZ78.

ABSTRACT 5G base stations usually use different beams to transmit broadcast and user data. Moreover the broadcast beam is always "on air", whilst the traffic beam is not. This represents a problem in Maximum Power Extrapolation (MPE) procedures for exposure assessment. In fact, currently adopted measurement approaches are based on the mere observation of phenomena. Recently, a different approach for MPE has been proposed by Adda *et al.*, 2020, forcing the traffic toward the measuring position by means of a dedicated User Equipment (UE). Consequently, the measurer loses the "passive" role assumed in the approach usually adopted, and acquires an active role forcing the system under test to assume the most suitable configuration. The use of beam-forcing UEs opens new exciting possibilities, since it makes it possible to take advantage of the *UE-specific signals* for the estimation for the MPE procedure. The aim of this paper is to explore the potential offered by UE-specific data structures within the MPE considering a real case regarding data acquired on a currently operative 5G base station.

INDEX TERMS 5G mobile communication, antennas, base stations, health and safety, MIMO.

I. INTRODUCTION

5G New Radio (NR) is characterized by new technical solutions at the physical level [2]. In particular, new sophisticated antenna solutions have been implemented to achieve a stable connection at an unprecedented high bit rate.

On the other hand, such a sophisticated technological solution poses a number of formidable new challenges in estimating the Electromagnetic Field (EMF) of 5G signals for human exposure assessment.

Loosely speaking, the approach currently investigated to handle this problem is based on two steps [3].

In the first step a proper procedure, called Maximum Power Extrapolation (MPE), allows to estimate the maximum possible field level radiated by the base station in the measurement point. The value obtained by the MPE procedure is an unrealistic upper bound, since it supposes that all the resources of the communication system are given to only one user. This quantity is then multiplied by a proper correction factor that takes into account the stochastic nature of the problem in order to obtain a realistic value [4]–[8].

Both problems represent thrilling challenges for researchers and technicians. This paper is focused on the 'first step', i.e. on the MPE procedure.

MPE is not a new problem and effective procedures have been developed and currently applied for previous

The associate editor coordinating the review of this manuscript and approving it for publication was Mingchun Tang.

generations of cellular communication systems. The standard MPE approach is based on identifying a constant power reference signal that is always present (i.e. it is ''always on''). For example, BCCH (Broadcast Control Channel) signal is used in GSM base stations, P-CPICH (Common Pilot Channel) is used in UMTS, while cell specific reference signal (CRS) is adopted as reference signal in LTE. All these signals are always transmitted with constant and maximum power.

The approaches proposed for MPE of 5G signals have been developed in continuity with the procedure conceived for previous generations of cellular systems.

However, 5G follows a different signaling strategy. In particular, it limits the ''always on'' signals as much as possible, packing all the fundamental information necessary for accessing the network in a signal structure highly concentrated in frequency, time and possibly space, called SS-PBCH. This is the only ''always on'' signal in NR, and consequently all proposed MPEs use the SS-PBCH as a reference [1], [9]–[14]. SS-PBCH has a number of other useful features, as it is transmitted at constant power and can be easily measured with high accuracy. For example, SSS and PBCH-DMRS, which are two reference signals proposed in 5G MPE procedures, can be measured using modern VNAs or network scanners.

The 5G standard gives a huge degree of flexibility to the vendor. In particular it is possible to use the same beam to transmit both the data of interest to all the users (f.i. the data in the SS-PBCH channel) and the data of interest to a specific user. This solution is commonly adopted in the DSS (Dynamic Spectrum Sharing) 5G systems, in which 5G shares the available resources with 4G, including antennas. For these systems measurement of the SS-PBCH is sufficient.

However, both for currently implemented non-standalone (NSA) 5G systems and for the upcoming standalone (SA) 5G systems, identifying a stable reference signal always in air does not completely solve the problem of MPE. In fact, 5G systems can use two different kinds of beams, the so-called 'broadcast' beam and the 'traffic' beam (see Fig. 1), whose directivity is different. In particular, the traffic beam is used to send payload data to the UE and has a greater directivity than the broadcast beam, which instead transmits information of interest to all users of the cell. Consequently, there is a power increase factor with respect to the power level measured using SS-PBCH that must be taken into account in MPE. At the best knowledge of the authors, this possibility is used in all the 5G NSA systems currently deployed.

Estimating the field radiated by the traffic beam is particularly complicated since it is not only a ''not always on'' signal, but it is also user-dependent and different users may be served by different traffic beams.

Most MPE approaches overcome the problem limiting the measurement to only the 'always on' signal, while the effect of the use of traffic beam is handled using a-priori information on the patterns of the broadcast beam and of the traffic beam. Following this approach, vendors make available information

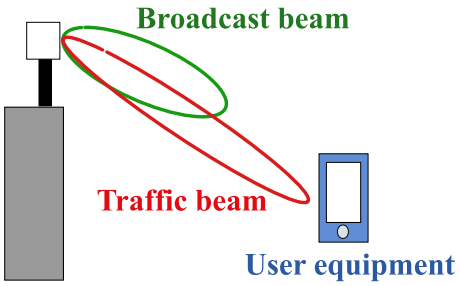

FIGURE 1. 5G uses two different kinds of grid of beams; the broadcast beams have lower directivity and are used to transmit signals of interest to all the UEs, as PSS, SSS and PBCH; traffic beams have higher directivity and are steered toward the UE to send UE-specific information, as PDSCH.

on the so called 'envelope of beams', that is basically the polar plot of the envelope of the Gain of the grid of beams, both for traffic and broadcast beams [15]. More complex approaches can be followed according also to the specific reference quantity chosen in the MPE procedure [16].

The evaluation of the uncertainty on the estimated field level using the envelop of beams data requires the estimation of two contributions. The first contribution is associated to the uncertainty affecting the envelop of beams data. The second one is related to the fact that measurements are usually carried out in a scattering environment. As well known, in this case the field in the measurement point is given by the interference of many contributions caused f.i. by reflections, refractions, diffraction phenomena, and the direct path in presence of LOS (Line of Sight) propagation. Observing Fig. 2, we can note that broadcast and data signals are subject to different propagation conditions depending on the illuminated area. Consequently the level of the field related to the broadcast beam in the measurement point is generally different from the one associated to traffic beams. This problem affects both NLOS propagation and, even if in less critical way, LOS propagation. Consequently, the power increase factor turns out to be different from the one calculated in case of free space propagation, making the evaluation of the uncertainty of the estimated MPE value a not straightforward task.

A further possible solution is to exploit the random positions of users actively connected to the base station. By recording the field level for a long enough time, there is a high probability that the measurement location is illuminated by one of the traffic beams [12].

The solution described above follows a traditional approach, in which the measurer is a passive observer, whose action is limited to the mere observation of phenomena.

Recently, a different approach for MPE has been proposed in [1]. Loosely speaking, the basic idea is to force the system in a state suitable for measuring the parameter of interest. In particular, the procedure followed in [1] forces the traffic toward the measurement position by means of a dedicated UE.

The use of UE-forcing devices opens new exciting possibilities, since it makes possible to take advantage of the *UE-specific signals* for the MPE procedure. In particular,

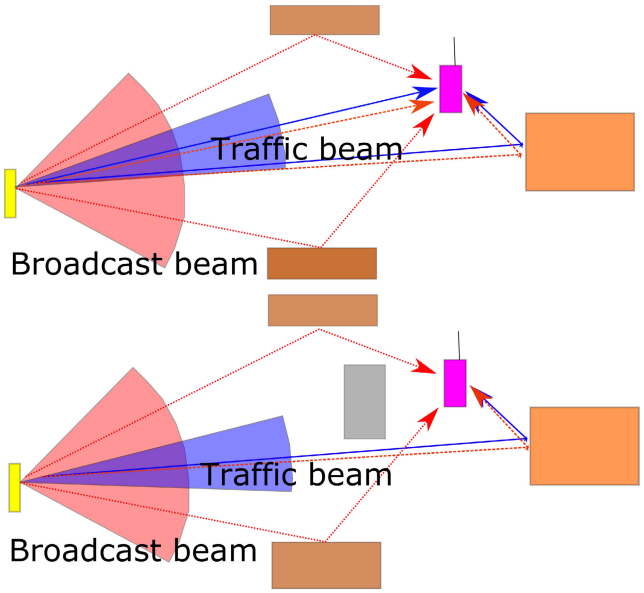

FIGURE 2. Example of LOS communication channel (upper figure) and NLOS communication channel (lower figure); in both cases different paths are associated to data beam and broadcast beam due to the different areas illuminated by the two beams; furthermore, also the paths that are common to broadcast and data beam give different contributions on the interference process since they have different amplitudes and phases according to the (complex, i.e. amplitude and phase) patterns of the data and broadcast antennas; this makes the estimation of the standard uncertainty from pattern data very cumbersome.

at the end of paper [1] it was suggested the possibility ''to take advantage of some data belonging to the rich set of signals associated to NR transmission'' and ''to extend the use of data signaling in the extrapolation procedure''.

The aim of this work is to explore the potential offered by UE-specific data structures within the MPE.

The paper is organized in the following way.

In Section II the problem of the power increase factor associated to the use of directive data beams is discussed.

In Section III methods based on the measurement of power of some portions of 5G frame are considered.

In Section IV methods based on measurement in the data domain are discussed.

In Section V conclusions are reported.

For the sake of reader convenience, the paper ends with an Appendix devoted to the analysis of 5G frame structure, with particular reference to the Physical Channel and Physical Signals.

As last observation, it is worth noting that the aim of this paper is limited to present a number of possible solutions for MPE offered by the use of beam-forcing devices. Even if no specific measurement procedure is proposed, the paper offers some indications regarding the most promising approaches. These approaches will be object of specific discussion in future papers.

II. TRAFFIC BEAM FIELD LEVEL AND MPE

The final goal of the Maximum Power Extrapolation procedure is the estimation of the maximum field level [V/m] that could be reached in the measurement point. We will call this quantity E_{5G}^{max} [1]. As indicated in the Introduction, this quantity is used as a reference to estimate the EMF exposure in realistic conditions by a suitable scaling factor.

While the details of the formulation can be different depending on the specific procedure proposed, the general approach is the same.

The method is based on a number of information on the structure of the frame, as bandwidth, numerology and duty cycle F_{TDC} in case of TDD transmissions. Such information allows to identify the number of REs available for the downlink transmission, let N_{sc} be. If not known a-priori, these quantities can be obtained by measurement.

Besides these quantities, the procedure requires the estimation of the maximum possible average EMF level associated to a RE, let E_{RE}^{max} be.

The maximum EMF level in the measurement location, is then estimated as

$$E_{5G}^{max} = \sqrt{N_{sc} F_{TDC}}\, E_{RE}^{max} \tag{1}$$

We must note that the actual measured quantity is the power at the connectors of the measurement equipment. It is possible to calculate the field amplitude E_{RE}^{max} from the power measurement P_{RE}^{max} using a calibrated antenna and cable:

$$E_{RE}^{max} = \sqrt{\frac{P_{RE}^{max} Z_{in}}{\alpha}} AF \tag{2}$$

wherein Z_{in} is the input impedance of the instrument, α is the cable attenuation and AF is the Antenna Factor of the antenna connected to the measurement equipment.

The goal is consequently the estimation of P_{RE}^{max}.

Control signals are transmitted on 'broadcast' beam or on 'traffic' beam (see Fig. 1) depending on their final use, as indicated in the previous Section. Broadly speaking, broadcast beams are used to transmit the SS/PBCH blocks, and in general signals of interest to all the users in the cell. According to the vendor choice, they can be transmitted on a fixed beam covering the entire sector of interest of the antenna, or, in more sophisticated implementations, using a 'grid of beams' allowing a 'spatially concentrated' transmission. The gain of these beams is relatively limited. Signals of interest to specific UEs are instead transmitted using ''traffic beams''. The higher directivity assures high signal/noise ratio on the user and better connection stability at high bit rate.

Clearly, P_{RE}^{max} is associated to traffic beams, that are 'user dependent' and cannot be measured without the presence of an active user in the measurement position.

The use of different beams causes the presence of a power increase factor between the maximum power per RE $P_{RE,max}^{ref}$ associated to the 'always on' signals used as reference (transmitted in the SS-PSBCH physical channel on the broadcast beam) and the maximum power per RE:

$$P_{RE}^{max} = P_{RE,max}^{ref} F_{beam} \tag{3}$$

wherein $P_{RE,max}^{ref}$ is the maximum received power level per RE of the signal selected as reference (f.i. the PBCH-DMRS

or the SSS) and F_{beam} is a parameter which takes into account the effect of the boost of the traffic beams due to beamforming and beamsweeping.

There are many possible procedures for the estimation of P_{RE}^{max}. In the following they will be divided into two categories according to the complexity and cost of the procedure: estimation from power measurement and estimation from data decoding. Details about the various signals recalled in next sections are given in the Appendix.

III. ESTIMATION FROM DIRECT POWER MEASUREMENT OF SELECTED PORTIONS OF 5G FRAME

In this Section we explore possible approaches based on the estimation of the maximum RE power of the PDSCH from power measurements directly on the 5G frame structure. The advantage of power measurement is that decoding of the signal is not required. Consequently, they can be carried out using both a vector spectrum analyzer or a less expensive scalar spectrum analyzer.

There is a number of control signals (i.e. not used to carry payload user data) that are suitable for the estimation of the maximum power per RE of the PDSCH (see the Appendix). As an example, the 5G frame, reported in the paper [1] and regarding a 4 layers (i.e. 4-subchannels SU-MIMO signal [17]), will be analyzed. In the example the scheduler was forced to send all the resources to the user that is placed in the measurement position. The interested reader is invited to refer to paper [1] for more information about the frame measurement procedure.

Figure 3 covers a frame, i.e. 10 ms. The numerology is $\mu = 1$, giving 2 slots of 0.5 ms each subframe, for a total of 20 slots per frame and 240 OFDM symbols. The void regions (no RE power) in the 7/8/9/17/18/19 slots are reserved for uplink data. The subcarriers spacing is 30 KHz, for a total of 2604 subcarriers and 80 MHz bandwidth.

The frame shown in Fig. 3 regards a case in which only one user has access to all the REs available for data transmission [1]. The figure shows the RE power [dB_{mW}] using a standard representation in VNA, known as ''Power vs. Symbol × Carrier'' plot. The x-axis represents the symbols while the y-axis represents the subcarriers. Different colors in the diagram area represent the power. A color map in the diagram header indicates the corresponding power levels.

On the left lower part the SS Block is clearly visible. It is transmitted with a 20 ms periodicity, and consists of 6 SS-PBCH. The beam associated to the third SSB is clearly received with highest power. The analysis of the SS-PBCH for a similar frame structure is reported in [1] and [10] and will not be repeated here. Instead this Section is devoted to the analysis of the remaining control signals.

The signaling structure after subtracting the PDSCHs and SS/PBCHs is shown in Fig. 4. We can note the PDCCH and PDCCH-DMRS signals in the CORESET area in the first OFDM symbol of each slot.

For sake of clarity, a block of 12 × 28 REs, i.e. a rectangle one RBs high and two slot long, is drawn in Fig. 5. In the

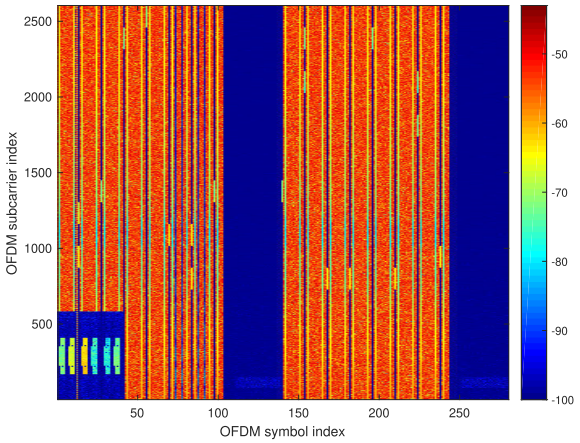

FIGURE 3. Power vs. symbol × Carrier map; the x-axis represents the symbols; the y-axis represents the subcarriers; different colors in the diagram area represent the power; a color map in the diagram header indicates the corresponding power levels in [dBm]; the communication system was forced to give all the resources to only one user.

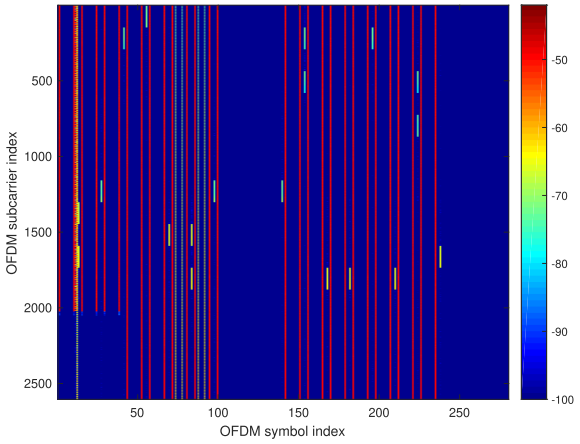

FIGURE 4. Signaling structure in a frame after subtracting SS Blocks and PDSCH REs; the RE power is drawn in false color according to the scale on the right (in [dBm]).

upper figure the power of the RBs is drawn in a false color scale (the scale in dBm is showed on the right). In order to clarify the positions of the REs used for data signaling, in the lower figure the signaling structure of the RBs is drawn in false color from 0 to 1. The REs used for PDSCH-DMRS are shown in code color 1 and 0.8 (red and orange, see the color scale on the right of the figure). The DMRS of the four PDSCHs are positioned at alternate frequency positions using two orthogonal coding according to a Mapping type A and Configuration Type 1 (see Appendix). Consequently, the amplitude of each RE in the PDSCH-DMRS reflects the superposition of the two signals associated to the two orthogonal coding's.

In the lower part of Fig. 5 the REs associated to the Tracking Reference Signal (TRS) are indicated using the color code 0.6 (yellow). As discussed in the Appendix, TRS is basically a highly dense version of Non Zero Power CSI-RS signal, and is transmitted on a single layer.

The other Non-Zero Power CSI-RS signals are transmitted using orthogonal coding. With reference to the right part

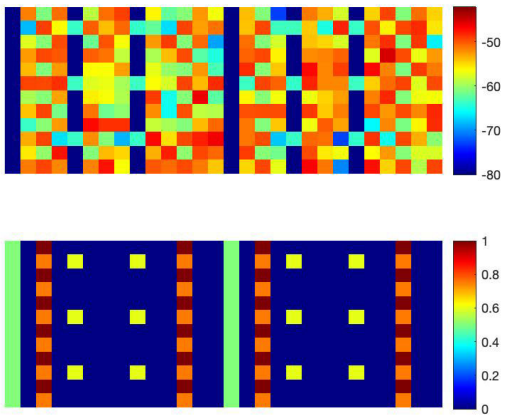

FIGURE 5. An example of two consecutive slots; in the upper figure the RE power is plotted in false colors, from −80 dBm to −40 dBm; it is possible to note some regular structures; these structures are associated to control signal's; in order to identify these structure in the lower figure the different functions of the related REs are plotted in false color according to the scale on the right; CORESET are plotted in green (color code 0.5 of the right color scale), PDSCH-DMRS are plotted in red bright and deep red (color codes 1 and 0.8), TRS are colored in yellow (color code = 0.6).

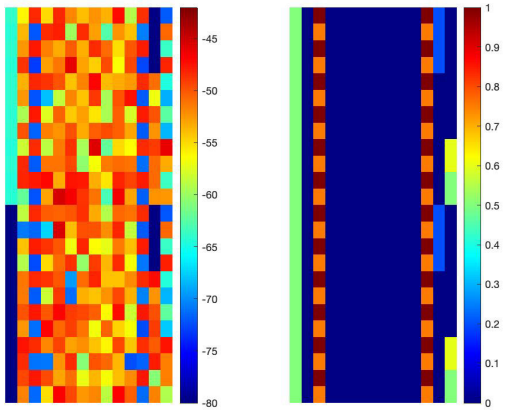

FIGURE 6. An example of two consecutive RBs; in the left figure the RE power is plotted in false colors, from −80 dBm to −40 dBm; it is possible to note some regular structures; these structures are associated to control signals; in order to identify these structures in the right figure the different functions of the RE are plotted in false color according to the scale on the right; CORESET are plotted in green (color code 0.5 of the right color scale), PDSCH-DMRS are plotted in red bright and deep red (color codes 1 and 0.8), NZP CSI-RS are colored in yellow and light green (color code = 0.6 and 0.55), ZP CSI-RS in light blue (color code 0.2).

of Fig. 6, the positions of the NZP CSI-RS are drawn in green (port 3000 and 3001) and in yellow (port 3002, 3003). The same figure shows also the position of ZP CSI-RS, that covers 4 REs drawn in light blue (color code 0.2). The power of the REs is shown in the left part of Fig. 6. It is interesting to note that the power level of the REs associated to ZP CSI-RS are drawn in deep blue color, indicating the absence of interference signals.

In order to show the effect of beamforming in the frame structure, as second example two users at large angular distance are present, one of them being in the measurement position [1]. In Fig.7 the power of the REs in a frame measured during the transmission is shown. The figure clearly shows two power levels of the PDSCHs associated to the two users, that are served by two different beams belonging to the grid of traffic beams [1]. The power level difference is also clearly shown in Fig. 8, reporting the REs power in two consecutive slots associated to different users.

Now, let us investigate the frame structure for the estimation of P_{RE}^{max}.

As first step, we evaluate the average power of all the downlink REs of the Power vs. Symbol × Carrier map. This value is plotted as a blue circle labelled as FR in Fig. 9, and represents a reference value.

A candidate for the estimation of the PDSCH is the PDSCH-DMRS. As discussed above, the measured data do not allow to distinguish the PDSCH-DMRS associated to the four ports from the available data. Consequently, we can estimate the P_{RE}^{max} from the PDSCH-DMRS associated to the ports 1000-1001 together, and the P_{RE}^{max} from the PDSCH-DMRS associated to the ports 1002-1003 together. The maximum of these values is plotted in Fig. 9 as blue circle labeled as PDSCH-DMRS. The estimated value is about 3dB higher than the others, which is due to the power boosting factor as reported in [18] Table 4.1-1.

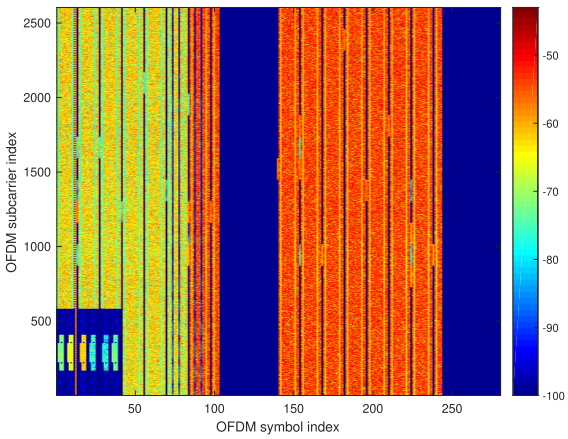

FIGURE 7. Power vs. symbol × Carrier map [dBm]; the communication system was forced to give all the resources to two users served by two different data traffic.

A further possibility is the estimation of the average value of PDSCH per RE directly from the measured data. In Fig. 9 the P_{RE}^{max} estimated from 1 RB and from 10 RBs considering different RBs in the RG are indicated as "PDSCH/1" and "PDSCH/10" labels.

Finally, for sake of completeness, the average value of the NZ CSI-RS REs not associated to the TRS has been also evaluated and labeled as CSI-RS in Fig. 9. This number gives an indication of the average power of the beams associated to the four layers in case of stable connection. However, it must be stressed that identification of CSI-RS requires information at Layer level higher than the Physical Layer. The CSI-RS configurations can be dynamically configured, and eventually also deactivated. Furthermore, the relationship between the

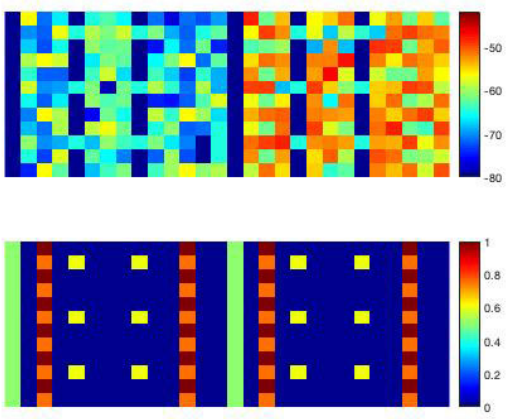

FIGURE 8. An example of two consecutive RBs associated to two different users served by two different data traffic; upper figure: RE power plotted in false colors, from −80 dBm to −40 dBm; lower figure: RBs structure (the different functions of the RE are plotted in false colors according to the scale on the right: CORESET = 0.5, PDSCH-DMRS = 1 and 0.8, NZP CSI-RS = 0.6 and 0.5, ZP CSI-RS = 0.2).

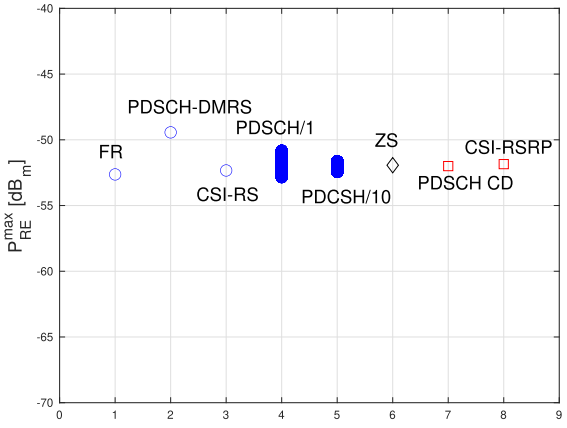

FIGURE 9. Estimated P_{RE}^{MAX} using different structures of the frame from power measurements: FR: value estimated using all the frame; DMRS-PBCH values obtained from PDSCH-DMRS REs power data; CSI-RS: values obtained from CSI-RS REs power data; PDSCH/1: values obtained from 1 PDSCH RBs power data; PDSCH/1010: values obtained from 10 PDSCH RBs power data; ZS: value obtained with Zero Span measurement; PDSCH CD: value obtained from PDSCH RE power measured in the Code Domain; CSI-RSRP: value obtained from CSI-RSRP.

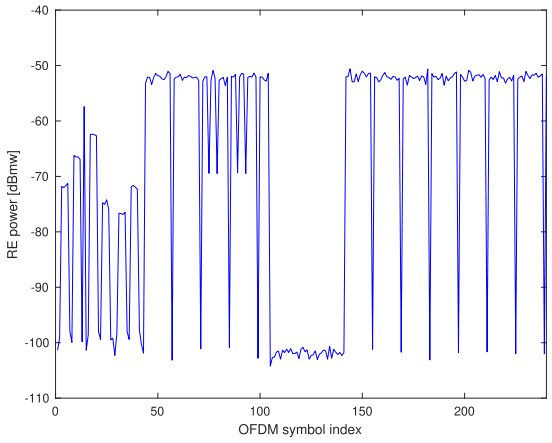

FIGURE 10. Span zero measurement procedure by scalar spectrum analyzer; the figure shows the power of the REs as obtained from a cut of the frame in a 1 MHz bandwidth with central bandwidth at the central frequency of the SS Burst.

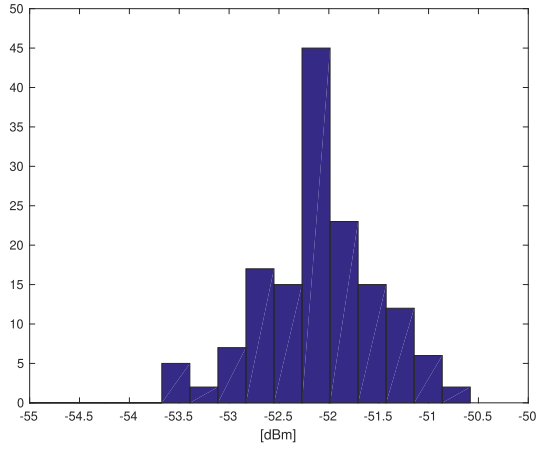

FIGURE 11. Statistical analysis of the REs power in the cut showed in Fig. 10 used to choose the RE power for the MPE method.

CSI-RS radiation pattern and the traffic beam depends on the number of configured CSI-RS.

As noted at the beginning of the subsection, the above analysis is based on 'power' measurements. Accordingly, provided that the structure of the frame is known, an expensive VNA with 5G software is not strictly required [1], [19].

As an example, in Fig. 10 the signal acquired by a scalar spectrum analyzer in zero span mode with 1 KHz RBW centered on the central frequency of the SSB is shown. The mode of the power of the REs associated to the traffic data forced toward the measurement position can be obtained by statistically analyzing the received data (see Fig. 11) [1], [12].

The value of the power per RE obtained with this procedure is plotted as a black diamond labeled as ZS in Fig. 9.

The results collected in Fig. 9 show that a direct measurement of the PDSCH RE power gives good results, while PDSCH-DMRS requires the knowledge of the associated power boosting factor to avoid overestimation in the MPE procedure [18].

Finally, the complexity of the CSI-RS structure as well as the highly dynamical flexibility in its use makes it necessary further studies on the practical effectiveness of the CSI-RS for MPE.

Before concluding this discussion, it is interesting to note that one of the main problems of power measurement is that the measurement system is not able to distinguish the field level associated to different cells since information on the ID of the PDSCH is missed. However, 5G intrinsically gives a method to have information on the interference level due to other cells. In fact, we can measure the power of the REs associated to the ZP CSI-RS, obtaining in this way a measure of the interference level. This can be obtained either by

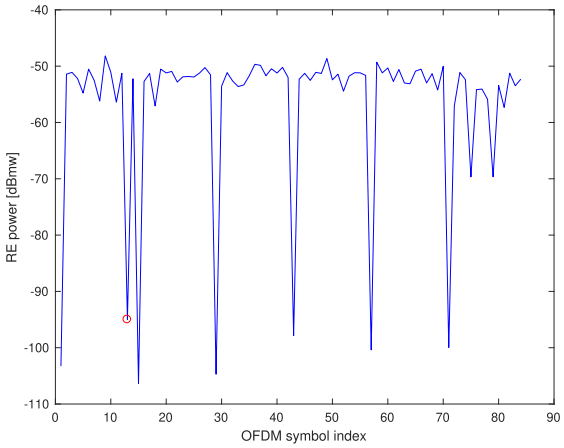

FIGURE 12. Span zero measurement procedure using a scalar spectrum analyzer; the figure shows the power of the REs as obtained from a cut of the frame in a 120 KHz (4 subcarrier spacing) bandwidth chosen to cover the ZP CSI-RS REs; the average REs of the ZP CSI-RS is indicated by a red circle, showing the absence of interference signal in the measured band; the other minima are related to CORESET not used by PDCCH.

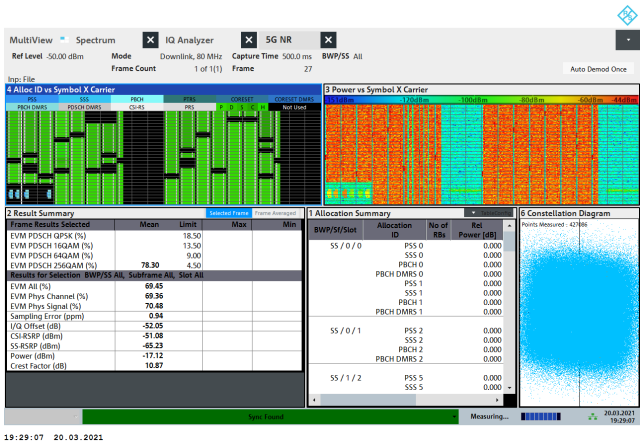

FIGURE 13. An example of VNA output; the power vs. symbol × Carrier map is drawn in the upper right window; allocation ID vs. symbol × carrier is drawn in the upper left window; the Allocation summary windows reported on the lower windows show various parameters of the measured allocations in a table.

a measurement of the power per RE on the power grid of the VNA, or also, at least theoretically, using a simpler scalar spectrum analyzer by selecting a RBW of the spectrum analyzer and a central frequency that covers the four consecutive REs of the ZP CSI-RS. As an example, in Fig 12 the signal on a 120 KHz (4 subcarrier spacing) bandwidth chosen to cover the ZP CSI-RS REs is shown. The average REs power level of the ZP CSI-RS is plotted as a red circle, indicating the absence of interference signal in the measured band (the other minima in the figures are related to CORESET not containing PDCCH). This information can be useful in power-based measurements since a low value of the ZP CSI-RS is an indication of the absence of other active cells, at least at the checked frequency, that could cause erroneous evaluation of the field level radiated by the cell under analysis. This check can be repeated also at other frequencies, since the ZP CSI-RS spreads over the entire frequency band.

IV. ESTIMATION IN THE CODE DOMAIN

Modern VNAs with 5G decoding, as well as modern 5G network scanners, allow to obtain a number of useful information potentially suitable for MPE procedure.

In Fig. 13 a typical output is shown (model: Rohde & Schwarz FSW26). The Power vs. Symbol × Carrier map is clearly identifiable in the upper right window. In the upper left window the "Allocation ID vs. Symbol × Carrier" result is reported. This map shows the allocation type of each subcarrier in each symbol of the received signal: the x-axis represents the OFDM symbols while the y-axis represents the subcarriers. Each type of identified allocation is represented by a different color. REs whose allocation is not identified are drawn in black.

The lower windows show the "Allocation Summary", that reports various parameters of the measured allocations. Each row in the allocation table corresponds to an allocation. Horizontal lines divide the slots. The columns of the table show a number of parameters for each allocation, as the location of the allocation (slot, subframe, bandwidth part number) and the ID of the allocation. In particular the fourth column shows the power per RE of each resource element in the allocation. In the figure the power per REs of the PSS, SSS, PBCH, PBCH-DMRS, PDSCH and PDSCH-DMRS are reported. Note that this is only a subset of the large range of information available on the measured allocations.

Accordingly, supposing that a UE forces the traffic toward the measurement position, modern VNAs are able to measure both the average PDSCH-DMRS power per RE and the average PDSCH power per RE of the data channel associated to the forcing UE. Note that the measurement of all the allocations of the frame is not required, since only the allocations carrying information to the forcing UE are of interest. This portion is supposed to have sufficiently high SIR level to be correctly decoded, since it is transmitted along the data beam pointing toward the forcing UE.

Regarding the data, the use of PDSCH-DMRS is less straightforward, since the PDSCH-DMRS power boosting factor compared to the PBSCH channel must be known, while the PDSCH power level gives a direct information on the P_{RE}^{max} by selecting the PDSCH power per RE of the strongest channel during the UE-forcing procedure.

As an example, the maximum value of the PDSCH reported in the Allocation Table is plotted in Fig. 9 as a red square labeled PDSCH CD (PDSCH Code Domain).

We conclude this brief review of possible approaches introducing the possibility to take advantage of the beam management procedure in 5G using the CSI-RS to obtain a direct information on the F_{beam} factor.

As preliminary step, we recall that UE performs three measurements to determine the signal quality of the surrounding NR cells:

- the Secondary Synchronization Reference Signal Received Power (SS-RSRP)

- the Secondary Synchronization Reference Signal Received Quality (SS-RSRQ)

- the Secondary Synchronization Signal Interference to Noise Ratio (SS-SINR)

In particular, the SS-RSRP is defined as the linear average over the power contributions (in Watt) of the resource elements carrying the Secondary Synchronization Signal (SSS). The SS-RSRP is used to compare the strengths of signals from individual cells in 5G networks, and is an important parameter for cell selection and handover. In fact, the measurement report for neighboring NR cells includes the identity of the cell, the RSRP, RSRQ and SINR for each cell, and the measurement result for each detected SSB listed by index with RSRP, RSRQ and SINR. The best SSB is reported first.

It is worth noting that DMRS and SS signals are transmitted with equal power, so the value of SS-RSRP can be also used to evaluate the PBCH-DMRS power per RE.

The NR cell quality assessment during initial access is based only on the SSS. However, after establishing the access, the CSI-RS can also be used. In particular, CSI-RS configured for beam management is used to choose the most suitable traffic beam by measuring the received power for each available beam, and hence gives information on the field level associated to the traffic beams.

The associated parameter of interest in the beam selection process is the Channel State Information Reference Signal Received Power (CSI-RSRP), defined as the linear average over the power contributions (in Watt) of the resource elements that carry CSI-RS configured for RSRP measurements within the considered measurement frequency bandwidth.

Summarizing, in downlink beam management, measurements can be performed by the UE on SSB or CSI-RS transmitted by the BS.

An example of CSI-RSRP measurement is also shown in Fig. 13. Information on the CSI-RS configuration has been acquired at the Layer 3 level using a network scanner. The CSI-RSRP value is reported in Fig. 9 as a red square labeled CSI-RSRP. Note that in the Result Summary window the SS-RSRP is also shown.

It is useful to recall that the use of CSI-RSRP is not mandatory, and in general CSI-RS can be dynamically reconfigured in a highly flexible way. This makes the practical use of CSI-RSRP and in general of CSI-RS for MPE not an easy task and understanding the practical utility of CSI-RSRP in MPE requires further investigation.

As last note, CSI-RSRP and SS-RSRP, can be obtained directly from a 5G phone. In fact, the software of a 5G mobile phone is optimized to decode all the complex control signals in real time, including for example the CSI-RS. Modern 5G network scanners, as well as software for data service quality supporting 5G technology, are able to access this information by using rooted cellular phones.

Even if the use of a cellular phone is attracting, it must be stressed that the data acquired by a mobile phone are not immediately useful for MPE procedure since the antenna factor of the cell phone receiver element is not known, as well as the gain/attenuation of the phone measurement chain. This would require a careful characterization of the phone in anechoic chamber, or in OTA (Over The Air) sites, using reference incident fields carrying 5G signals. However, such a characterization is quite complex, and further research on the practical applicability of such a solution must be carried out.

V. CONCLUSION

The use of UE terminals able to force the traffic toward the measurement direction allows to take advantage of the rich set of 5G data signals. In this paper the potential offered by UE-specific data structures, as PDSCH-DMRS and PDSCH is explored with reference to the MPE problem, considering both solutions based on power measurement and on information collected in the code domain. The results show that the use of beam-forcing UEs allows for many effective solutions to the problem of MPE.

In conclusion, direct measurement of the power of the REs of the PDSCH channel appears to be a relatively simple and effective solution, and research on this approach. is currently carried out.

Finally, the feasibility of other solutions, as the use of CSI-RSRP, require further investigation.

As last observation, it is useful to stress that a key point in the measurement procedure is the use of a UE able to actively interact with the base station.

Put simply, 5G systems are characterized by unprecedented flexibility in terms of beam management. This presents a huge problem in MPE as measurements are performed in unknown beam states. The use of a UE device capable of actively interacting with the base station allows to force the system into a state suitable for measurement.

This document focuses on the systems currently implemented. In the future, the use of MU-MIMO will increase the complexity of the measurement by increasing the number of possible states in terms of pattern configurations. The use of UEs that can actively interact with the base station could help to force measurements into some specific states suitable for measurement.

The approach described in this paper allows also to investigate solutions that significantly deviate from the ones currently adopted for MPE. For example, the possibility to have a controlled access to the power of the traffic beam resource element opens new measurement scenarios in which the 'always on' reference signal loses its centrality.

In this sense, this paper must be considered only a timid first exploration of a world of enormous potential of innovation.

APPENDIX
OVERVIEW OF THE 5G FRAME STRUCTURE

In this Appendix some characteristics of the frame structure of 5G signals are reported. We will not enter into the details of 5G signals, for which the reader is invited to refer to 3GPP group reports and standards [2]. Instead, this Section will be

focused on the understanding of some aspects of 5G signal relevant for the measurement of the electromagnetic field level.

Regarding the use of the frequency resources, NR supports two bandwidths: Frequency Range 1 (FR1), commonly referred to as sub-6 GHz, ranging from 410 MHz to 7.125 GHz, and Frequency Range 2 (FR2), commonly referred to as millimeter wave, ranging from 24.250 GHz up to 52.600 GHz. In this paper we will focus our attention on the FR1, that is the frequency band used by most currently deployed systems. Orthogonal Frequency-Division Modulation (OFDM) and Cyclic Prefix with variable subcarrier spacing and OFDM-symbol duration is used. A NR carrier is made of up to 3276 subcarriers. The maximum bandwidth of each NR carrier is 100 MHz for sub-6 GHz band (FR1) and 400 MHz for millimeter band (FR2). NR allows to configure up to four bandwidth parts (BWP), wherein a bandwidth part is a subset of contiguous subcarriers. This allows to choose different bandwidths according to the request of the UE.

Regarding the use of the time resources, the time length of the NR frame is 10 ms and consists of 10 subframes, with a time length of 1 ms each. 5G NR uses a ''flexible numerology'' characterized by the parameter μ. Each NR subframe contains 2^{μ} slots, where μ can be 0, 1, 2, 3 or 4. Each slot period (having $1/2^{\mu}$ ms time duration) contains 14 OFDM symbols (12 OFDM symbols in case of extended cyclic prefix). Consequently, the symbol duration is reduced according to the numerology [2].

Different numerologies are associated to different OFDM subcarrier spacings. In particular, the subcarrier spacing turns out to be $2^{\mu} \cdot 15$ KHz. At ''data'' level, the smallest physical resource is represented by 1 subcarrier and 1 OFDM symbol and defines a ''Resource Element'' (RE). 12 consecutive subcarriers in the frequency domain constitute a Resource Block (RB), while the RBs and OFDM symbols in a subframe define a Resource Grid (RG).

With reference to the use of the space resources, 5G communication is largely based on the use of beamforming and spatial multiplexing techniques including SU-MIMO and MU-MIMO. The ability to transmit independent information using the same time/frequency resources using different communication layers is quantified in the concept of ''antenna port'', defined by 3GPP ''such that the channel over which a symbol on the antenna port is conveyed can be inferred from the channel over which another symbol on the same antenna port is conveyed''. In practice, each antenna port is associated to a resource grid and a specific set of reference signals in the grid, allowing the reuse of the space-time resources of the channel. Different ranges of numbers are associated to ports used for different purposes:

1) PDSCH: Antenna ports starting with 1000
2) PDCCH: Antenna ports starting with 2000
3) CSI-RS: Antenna ports starting with 3000
4) SS/PBCH: Antenna ports starting with 4000

The relationship between the concept of antenna port at the Physical Layer level and at the ''Deep Physical Layer'' level (i.e. at the level of the field configurations, [20]), is discussed for example in [1]. Loosely speaking, the maximum number of layers that we can obtain at the Physical Layer level is limited by an electromagnetic quantity, called the Number of Degrees of Freedom of the field at the ϵ-level (ϵ-NDF, [20], [21]). An interactive simulation of the impact of MIMO antennas in the field level is reported in [22].

Before discussing the Physical Channels and Signals, let us introduce the general structure of a 5G frame.

The structure has been conceived to obtain high energy efficiency, and NR avoids as much as possible ''always on air'' signals. Consequently, the fundamental pieces of information that are required by the UE for initial connection to the cell are 'packed' in a very compact structure, called the Synchronization Signal / Physical Broadcast Channel (SS/PBCH), or ''SS Block'' (SSB), that includes the Synchronization Signals (SS), the PBCH and the PBCH-DMRS. SSB is mapped into 4 OFDM symbols in the time domain and 240 contiguous subcarriers (20 RBs) in the frequency domain.

SS Blocks are grouped in block patterns called SS bursts. There are 5 block patterns which have different subcarrier spacings and are applicable for different carrier frequencies: Case A (15 KHz subcarrier spacing), Case B (30 KHz subcarrier spacing), Case C (30 KHz subcarrier spacing), case D (120 KHz subcarrier spacing) and Case E (240 KHz subcarrier spacing). The maximum number of SS blocks in a single burst is frequency dependent, and ranges from 4 or 8 in FR1 to up to 64 blocks per burst in FR2. Each SSB in a SS Burst is associated to a different beam of the grid of broadcast beams.

The other signals are transmitted when required. They are usually transmitted on traffic beams and, loosely speaking, are ''user-dependent''. 5G uses a sophisticated signaling structure. In this paper we have limited our discussion on the physical channels and signals associated to downlink connection.

The choice of the beam (broadcast or traffic) on which the signals are transmitted is generally left to the vendor decision. In the following the most common choices are indicated.

A. PHYSICAL CHANNELS

The Physical Channels defined in downlink are

1) The Physical Broadcast Channel (PBCH).
2) The Physical Downlink Shared Channel (PDSCH).
3) The Physical Downlink Control Channel (PDCCH).

Each Physical Channel has its own Demodulation Reference Signal (DMRS) for channel estimation and equalization, as discussed in the following Subsections.

1) THE PHYSICAL BROADCAST CHANNEL (PBCH)

PBCH carries basic system information required to access the network, and in particular the Master Information Block (MIB). The PBCH is transmitted using QPSK in the PBCH-SS blocks with its own demodulation reference signal

using broadcast beams. NR supports only one antenna port based transmission for PBCH data in order to avoid blind decoding.

2) THE PHYSICAL DOWNLINK CONTROL CHANNEL (PDCCH)

The PDCCH provides scheduling decisions necessary for the reception of PDSCH, as well as special purposes such as slot format indication and power control. The information carried by the PDCCH is referred to as Downlink Control Information (DCI).

PDCCH is transmitted in a CORESET (COntrol REsource SET) using QPSK modulation. A CORESET is a set of resource blocks which has varying time and frequency domain length. In time domain it may occupy 1, 2 or 3 OFDM symbols whereas in frequency domain it is a multiple of one resource block (12 subcarriers). Loosely speaking, CORESET defines a resource where UE specific scheduling information can occur.

PDCCH has its own PDCCH-DMRS signal, and is transmitted on traffic beams.

3) THE PHYSICAL DOWNLINK SHARED CHANNEL (PDSCH)

This is the main channel used for data transmission, paging information, some parts of system information and also random-access response message. It decodes DCI from PDCCH which provides the necessary information to decode data in PDSCH.

The frequency resource allocation is organized in resource blocks, with flexible modulation schemes selected on the basis of the SNR.

PDSCH has its own PDSCH-DMRS signal, and is transmitted on traffic beams.

B. PHYSICAL SIGNALS

Physical channels carry information originating from the higher layers. In addition, 5G NR defines additional physical signals that do not carry information from higher layers, but are used for functionalities like synchronization, channel estimation, tracking and beam identification.

The physical signals defined in dowlink are:

1) The Primary Syncronization Signal (PSS) and Secondary Synchronization Signal (SSS)
2) The Physical Broadcast Channel Demodulation Reference Signal (PBCH-DMRS)
3) The Physical Download Control Channel Demodulation Reference Signal (PDCCH-DMRS)
4) The Physical Download Shared Channel Demodulation Reference Signal (PDSCH-DMRS)
5) Phase Tracking Reference Signal (PTRS)
6) The Channel-state Information reference signal (CSI-RS)

1) THE PRIMARY SYNCHRONIZATION SIGNAL AND SECONDARY SYNCHRONIZATION SIGNAL (PSS, SSS)

PSS and SSS play a key role in synchronization and cell search. PSS helps to achieve subframe, slot and symbol synchronization in the time domain, identify the center of the channel bandwidth in the frequency domain and deduce a pointer to 1 of 3 Physical layer Cell Identities (PCI). SSS helps to achieve radio frame synchronization and deduce a pointer to 1 of 168 Physical layer Cell Identity (PCI) groups.

PSS and SSS are transmitted in the SS-PBCH block using BPSK constellation on broadcast beams with constant power, so they are suitable as reference signals. SSS has been proposed as reference signal in [13], [16].

2) THE PBCH-DMRS

PBCH-DMRS is a special type of physical layer signal used as reference signal for decoding PBCH. PBCH-DMRS is transmitted in the SS-PBCH block using broadcast beams with constant power and is transmitted also in absence of users. It is one of the signals proposed as reference in MPE techniques [1].

3) THE PDCCH-DMRS

PDCCH-DMRS is a special type of physical layer signal used as reference signal for decoding PDCCH. It is transmitted together with the PDCCH in a CORESET using traffic beams.

NR considers the possibility of a power boosting factor for the PDCCH-DMRS. In particular 3GPP defines the β_{PDCCH}^{DMRS} factor as the ratio between PDCCH Energy per Resource Element (EPRE) and PDCCH-DMRS EPRE.

4) THE PDSCH-DMRS

PDSCH-DMRS has a 'double role' in PDSCH decoding. In fact, NR assumes that precoding is used for data. PSDSCH-DMRS is transmitted on traffic beams using the same precoding of the data, allowing to estimate both the response of the propagation channel and the precoding.

The position of the PDSCH-DMRS is characterized by a high degree of flexibility in order to match the characteristics of the communication channel and of the user application.

In particular, PDSCH-DMRS is mapped in PDSCH RB according to Mapping Type A or B and Configuration Type 1 or 2. The Mapping Type A or B defines the mapping location in the slot. In Type A the DRMS allocation is in the symbol 2 or 3, while in Type B the DMRS is allocated in the first symbol of PDSCH allocation, and is used when the PDSCH covers only a part of the slot, allowing a fast demodulation of the data required for low latency applications. The DMRS Configuration Type 1 or 2 specifies the density of the DRMS. Type 1 is denser in frequency, while Type 2 supports a larger number of orthogonal DMRS sequences, required to handle a large number of MIMO layers as in MU-MIMO.

The minimum number of DMRS symbols per slot is 1, but it is possible to add up to 3 additional DMRS symbols per slots to handle critical synchronization scenarios as high speed applications. In case of multiple layers transmission, DMRS uses different locations in frequency domain to allocate the ports. Two orthogonal pseudo-noise sequences are used to map two antenna ports on the same frequency,

allowing to half the number of frequencies. Taking into account that each symbol can be associated to two different codes, that DMRS can be allocated in a single symbol or in a double symbols configurations, and that Type 1 has two possible locations in the frequency domain while Type 2 can have four different positions, we have that Type 1 can supports only up to 4 orthogonal signals for single symbol DMRS, or 8 orthogonal symbols for double symbols, while Type 2 supports up to 6 orthogonal signals for each DMRS symbol, or 16 in double symbols configuration.

Finally, NR considers the possibility of a power boosting factor associated to the EPRE. In particular 3GPP defines the β_{DMRS} factor as the ratio between PDSCH EPRE and DMRS EPRE.

5) PHASE TRACKING REFERENCE SIGNALS (PTRS)

PTRS can be optionally used in PDSCH channel for compensating the phase noise and is particularly important in FR2, where phase noise is an important problem. It is sparser in frequency and denser in time as compared to DMRS.

5G introduces a power boosting factor associated to the EPRE. In particular 3GPP defines the β_{PTRS} factor as the ratio between PTRS EPRE and PDSCH EPRE.

6) CHANNEL STATE INFORMATION-REFERENCE SIGNAL (CSI-RS)

CSI-RS is used by the device to acquire information about the downlink channel. It is decoded by the device and sent as feedback to the base station as part of reports via PUSCH and PUCCH uplink channels. In particular, CSI reports consist of three parameters: RI (Rank Indicator), PMI (Precoding Matrix Index) and CQI (Channel Quality Information). The Rank Indicator indicates how many independent layers can be transmitted by the base station. The Precoding Matrix Indicator indicates what precoding matrix should be used by the transmitter for beam-forming on the base of a codebook of precoded matrices. Finally, CQI gives information on the quality of the communication channel. Based on the report, the base station optimizes various parameters like the number of transmission layers, modulation and coding scheme, and the pre-coding matrix to be used. The CSI report only provides suggestions and the transmitter is free to decide whether to follow the recommendation included in the report.

The CSI-RS resources can be allocated in three ways, namely in a periodic, semi-persistent or aperiodic basis. Semi-persistent is equivalent to periodic configuration, the only difference being that the activation and deactivation of CSI-RS transmission are controlled by MAC. Not all kinds of combinations among periodicity types for measurement and reporting are allowed.

CSI-RS can have a frequency density equal to 1 in which case it will be transmitted in every resource block for the full bandwidth, or density of 1/2 in which case it will be transmitted in alternate resource blocks.

In a multi-port, the separation is achieved by modulating with different orthogonal codes, by separating in frequency, or by separating in time.

The CSI-RS can be Non Zero Power (NZP) or Zero Power (ZP, or Muted). The NZP REs are associated to a no-transmission condition. This allows to use the frequency-time resources associated to a ZP CSI-RS to estimate the interference level due for example to the presence of other cells active on the same bandwidth.

Finally, there is also a third kind of CSI-RS with 3 subcarriers for each RB. This kind of CSI-RS is very dense in frequency and is used for the Tracking Reference Signal (TRS). On the contrary of the other CSI-RS transmissions, the TRS is single port.

In practice, the high flexibility of CSI-RS allows to configure it for multiple purposes, as TRS, CSI acquisition, and beam management. This last configuration is particularly interesting in the framework of MPE procedures since it can be used to obtain UE-specific information.

ACKNOWLEDGMENT

The authors would like to thank Dr. Roberto Cosentino and Dr. Massimo Bauco (Rohde Schwarz company) for the useful discussion on the equipment for 5G signal measurement.

REFERENCES

[1] S. Adda, T. Aureli, S. D'Elia, D. Franci, E. Grillo, M. D. Migliore, S. Pavoncello, F. Schettino, and R. Suman, "A theoretical and experimental investigation on the measurement of the electromagnetic field level radiated by 5G base stations," *IEEE Access*, vol. 8, pp. 101448–101463, 2020.

[2] *Radio Transmission and Reception (Release 15), 3GPP Technical Specification Group Radio Access Network*, Standard Nr, TS 38.104, v15.5.0, 3GPP, May 2019.

[3] *Determination of RF Field Strength, Power Density and SAR in the Vicinity of Radiocommunication Base Stations for the Purpose of Evaluating Human Exposure*, document IEC 62232:2017, Internation Electromechanical Commission, 2017.

[4] P. Baracca, A. Weber, T. Wild, and C. Grangeat, "A statistical approach for RF exposure compliance boundary assessment in massive MIMO systems," in *Proc. 22nd Int. ITG Workshop Smart Antennas (WSA)*, Mar. 2018, pp. 1–6.

[5] B. Thors, A. Furuskär, D. Colombi, and C. Törnevik, "Time-averaged realistic maximum power levels for the assessment of radio frequency exposure for 5G radio base stations using massive MIMO," *IEEE Access*, vol. 5, pp. 19711–19719, 2017.

[6] D. Pinchera, M. D. Migliore, and F. Schettino, "Compliance boundaries in 5G communication systems: A statistical approach," *EEE Access*, vol. 1, no. 1, pp. 620–628, 2020.

[7] D. Colombi, P. Joshi, B. Xu, F. Ghasemifard, V. Narasaraju, and C. Törnevik, "Analysis of the actual power and EMF exposure from base stations in a commercial 5G network," *Appl. Sci.*, vol. 10, no. 15, p. 5280, Jul. 2020.

[8] M. D. Migliore and F. Schettino, "Power reduction estimation of 5G active antenna systems for human exposure assessment in realistic scenarios," *IEEE Access*, vol. 8, pp. 220095–220107, 2020.

[9] H. Keller, "On the assessment of human exposure to electromagnetic fields transmitted by 5G NR base stations," *Health Phys.*, vol. 117, no. 5, pp. 541–545, 2019.

[10] D. Franci, S. Coltellacci, E. Grillo, S. Pavoncello, T. Aureli, R. Cintoli, and M. D. Migliore, "Experimental procedure for fifth generation (5G) electromagnetic field (EMF) measurement and maximum power extrapolation for human exposure assessment," *Environments*, vol. 7, no. 3, p. 22, Mar. 2020.

[11] D. Franci, S. Coltellacci, E. Grillo, S. Pavoncello, T. Aureli, R. Cintoli, and M. D. Migliore, "An experimental investigation on the impact of duplexing and beamforming techniques in field measurements of 5G signals," *Electronics*, vol. 9, no. 2, p. 223, Jan. 2020.

[12] S. Aerts, L. Verloock, M. Van Den Bossche, D. Colombi, L. Martens, C. Törnevik, and W. Joseph, "*In-situ* measurement methodology for the assessment of 5G NR massive MIMO base station exposure at sub-6 GHz frequencies," *IEEE Access*, vol. 7, pp. 184658–184667, 2019.

[13] A.-K. Lee, S.-B. Jeon, and H.-D. Choi, "EMF levels in 5G new radio environment in Seoul, Korea," *IEEE Access*, vol. 9, pp. 19716–19722, 2021.
[14] S. Aerts, K. Deprez, D. Colombi, M. Van den Bossche, L. Verloock, L. Martens, C. Törnevik, and W. Joseph, "*In situ* assessment of 5G NR massive MIMO base station exposure in a commercial network in Bern, Switzerland," *Appl. Sci.*, vol. 11, no. 8, p. 3592, Apr. 2021.
[15] N. Alliance, "Recommendation on base station active antenna system standards," NGMN Alliance, Frankfurt, Germany, Tech. Rep. 1.0, Jan. 2020. [Online]. Available: https://ngmn.org/wp-content/uploads/Publications/2020/NGMN_BASTA-AA_WP_1_0.pdf
[16] "Technical report: Measurement method for 5G NR base stations up to 6 GHZ," Federal Inst. Metrol., Swiss, Tech. Rep. 2.1, Feb. 2020. [Online]. Available: https://www.metas.ch/dam/metas/de/data/dokumentation/rechtliches/nisv/Nr_measurement_methods_2_1_en.pdf.download.pdf/Nr_measurement_methods_2_1_en.pdf
[17] M. D. Migliore, "The world beneath the physical layer: An introduction to the deep physical layer," *IEEE Access*, vol. 9, pp. 77106–77126, 2021.
[18] *Physical Layer Procedures for Data (Release 15), 3GPP Technical Specification Group Radio Access Network*, Standard NR, TS 38.214, v15.3.0, 3GPP, Oct. 2018.
[19] D. Colombi, P. Joshi, R. Pereira, D. Thomas, D. Shleifman, B. Tootoonchi, B. Xu, and C. Tornevik, "Assessment of actual maximum RF EMF exposure from radio base stations with massive MIMO antennas," in *Proc. Photon. Electromagn. Res. Symp. Spring (PIERS-Spring)*, Jun. 2019, pp. 570–577.
[20] M. D. Migliore, "On electromagnetics and information theory," *IEEE Trans. Antennas Propag.*, vol. 56, no. 10, pp. 3188–3200, Oct. 2008.
[21] M. D. Migliore, "Horse (electromagnetics) is more important than horseman (information) for wireless transmission," *IEEE Trans. Antennas Propag.*, vol. 67, no. 4, pp. 2046–2055, Apr. 2019.
[22] *Web Site*. Accessed: Mar. 1, 2021. [Online]. Available: https://sites.google.com/unicas.it/electromagnetic-information/home

MARCO DONALD MIGLIORE (Senior Member, IEEE) received the Laurea degree (Hons.) and the Ph.D. degree in electronic engineering from the University of Naples, Naples, Italy. He was a Visiting Professor at the University of California at San Diego, La Jolla, CA, USA, in 2007, 2008, and 2017; the University of Rennes I, Rennes, France, in 2014 and 2016; the Centria Research Center, Ylivienka, Finland, in 2017; the University of Brasilia, Brazil, in 2018; and the Harbin Technical University, China, in 2019. He was a Speaker at the Summer Research Lecture Series of the UCSD CALIT2 Advanced Network Science, in 2008. He is currently a Full Professor at the University of Cassino and Southern Lazio, Cassino, Italy, where he is also the Head of the Microwave Laboratory and the Director of studies of the ITC courses. He is a member of the ELEDIA@UniCAS Research Laboratory and the National Interuniversity Research Center on the Interactions between Electromagnetic Fields and Biosystems (ICEMmB), where he is the Leader of the 5G Group, the Italian Electromagnetic Society (SIEm), and the (National Interuniversity Consortium for Telecommunication (CNIT). His current research interests include the connections between electromagnetism and information theory, the analysis, synthesis and characterization of antennas in complex environments, antennas and propagation for 5G, *ad-hoc* wireless networks, compressed sensing as applied to electromagnetic problems, and energetic applications of microwaves. He serves as a referee for many scientific journals and has served as an Associate Editor for IEEE TRANSACTIONS ON ANTENNAS AND PROPAGATION.

DANIELE FRANCI received the M.Sc. degree *(cum laude)* and the Ph.D. degree in nuclear and subnuclear physics from the Sapienza University of Rome, Italy, in 2007 and 2011, respectively. From 2009 to 2011, he was an Analyst Technologist with Nucleco SPA involved in radiological characterization of radioactive wastes from the decommissioning of former Italian nuclear power plants. In 2011, he joined ARPA Lazio, being involved in RF EMF human exposure assessment. Since 2017, he has been involved in activities of CEI for the definition of technical procedures for EMF measurement from 4G/5G mMIMO sources.

SETTIMIO PAVONCELLO was born in Rome, Italy, in 1973. He received the M.Sc. degree in telecommunication engineering from the Sapienza University of Rome, Italy, in 2001. Since 2002, he has been working for Regional Environmental Agency of Lazio in Rome EMF Department. He is specialized in electromagnetic field measurements and EMF projects evaluation related to radio, TV, and mobile communications systems maturing huge experience in the use of broadband and selective instruments. In last years, he has deepened the issues related to measurements on LTE and NB-IoT signals. Since 2018, he has been actively involved in the working group of the Italian Electrotechnical Committee aimed at defining measurement procedures for mobile communications signals and is currently engaged in various projects concerning measurement on 5G signals.

ENRICO GRILLO received the M.Sc. degree in electronics engineering from the Seconda Università di Napoli, Aversa, Italy, in 1999. In 2000, he works as a RF to grow up the first 3G telecommunication radio network. Since 2005, he has been involved as a Research Technician in prevention and monitoring of electromagnetic pollution at ARPA Lazio, the local environmental agency of the Lazio.

TOMMASO AURELI received the M.Sc. degree in biological science from Sapienza University, Rome, Italy, in 1985. He joined ARPA Lazio, in 2002. From 2004 to 2018, he was the Director of the EMF Divison, being involved in both measurement and previsional evaluation EMF from civil sources. He is currently the Director of the Department of Rome.

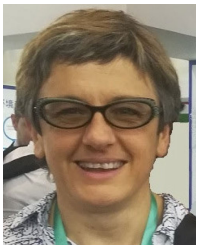

SARA ADDA received the M.Sc. degree *(cum laude)* in physics and the postgraduate specialization degree in health physics from Turin University, Italy, in 1998 and 2003, respectively. She worked for one year, from 1998 to 1999, at ENEA Casaccia, Rome, within the Interdepartmental Computing and High Performance Networks project, implementing a system for the simulation of electromagnetic field dynamics in complex environments through the use of massively parallel architectures. Since 1999, she has been working with the Physical and Technological Risk Department, ARPA Piedmont, dealing with control and monitoring of non-ionizing radiation and the development of theoretical forecasting/numerical calculation methods, both in the low and high frequency ranges. She also participates in the Italian Electrotechnical Committee (CEI) working groups, for the drafting of technical standards on measurement and evaluation methods for human EMF exposure, and she deals with the theoretical and practical aspects related to the measurement of electromagnetic fields in the workplace. In this context, she is the representative of the Interregional Technical Coordination Group, Piedmont. She participates in European (Twinning Italy-Poland project) and international collaborative projects (Arpa Piemonte—Beijing Municipal Environmental Protection Bureau), on methods and techniques for measuring and evaluating human exposure to EMF both in the workplace and in the living environment.

RICCARDO SUMAN was born in Ivrea, Italy, in 1974. He received the B.Sc. degree in telecommunication engineering from the Politecnico di Torino, Italy, in 1996. Since 1996, he has been with Vodafone Italy (formerly Omnitel Pronto Italia) where he is currently working as an Antenna Matter Expert. He also participates in the BASTA AA (Recommendation on Base Station Active Antenna Standards) by NGMN Alliance. Since 2012, he has been involved in activities related to EMF focusing on measuring and modeling electromagnetic fields and electromagnetic exposure assessment of base stations for mobile communications. He also participates in the Technical Committee 106 of the Italian Electro Technical Committee (CEI) and as a National Delegate in the IEC TC106.

STEFANO D'ELIA received the M.Sc. degree *(cum laude)* in electronic engineering from the University of Rome "La Sapienza." He joined Vodafone Italy (formerly Omnitel Pronto Italia) in 1998. Since 2002, he has been the Convenor of the working group "Mobile Base Stations" within the Technical Committee 106 of the Italian Electro Technical Committee (CEI), acting as a national delegate in several standardization bodies on EMF measurements and calculations. In 2012, he was awarded as a Vodafone Distinguished Engineer, one of the highest steps in the technical career path at Vodafone, where he is currently covering the role of Mobile Access Integrated Solutions Manager in group networks.

FULVIO SCHETTINO (Senior Member, IEEE) received the Laurea degree (Hons.) and the Ph.D. degree in electronic engineering from the University of Naples, Naples, Italy. He is currently an Associate Professor at the University of Cassino and Southern Lazio, Cassino, Italy. He is a member of the ELEDIA@UniCAS Research Laboratory, the National Interuniversity Research Center on the Interactions between Electromagnetic Fields and Biosystems (ICEMmB), the Italian Electromagnetic Society (SIEM), and the National Interuniversity Consortium for Telecommunication (CNIT). His current research interests include numerical electromagnetics, regularization methods, the connections between electromagnetism and information theory, the analysis, synthesis and characterization of antennas in complex environments, antennas and propagation for 5G, and energetic applications of microwaves.